Optics Letters

Self-referenced octave-wide subharmonic GaP optical parametric oscillator centered at 3 μm and pumped by an Er-fiber laser

Qitian Ru,[1,*] Zachary E. Loparo,[2] XiaoSheng Zhang,[3] Sean Crystal,[1] Subith Vasu,[2] Peter G. Schunemann,[4] and Konstantin L. Vodopyanov[1]

[1]CREOL, College of Optics and Photonics, University of Central Florida, Orlando, Florida 32816, USA
[2]Mechanical and Aerospace Engineering, University of Central Florida, Orlando, Florida 32816, USA
[3]State Key Laboratory of Precision Measurement Technology and Instruments, Department of Precision Instrument, Tsinghua University, Beijing 100084, China
[4]BAE Systems, P. O. Box 868, MER15-1813, Nashua, New Hampshire 03061-0868, USA
*Corresponding author: qitian@knights.ucf.edu

Received 2 October 2017; accepted 12 October 2017; posted 17 October 2017 (Doc. ID 307987); published 14 November 2017

We report an octave-wide mid-IR spectrum (2.3–4.8 μm) obtained from a subharmonic optical parametric oscillator (OPO) based on a newly developed nonlinear crystal, orientation-patterned gallium phosphide (OP-GaP), which was synchronously pumped by a femtosecond 1560 nm fiber laser. We proved that the octave-wide output is in the form of a single frequency comb. The observed *f*-to-2*f* frequency beats, originating directly from the OPO, can be used for self-referencing and phase locking of the pump laser comb with no need for supercontinuum generation. With an average output power of ~30 mW, this setup might be beneficial for a variety of spectroscopic applications in the mid-IR.

OCIS codes: (190.4975) Parametric processes; (190.4410) Nonlinear optics, parametric processes; (320.7110) Ultrafast nonlinear optics.

https://doi.org/10.1364/OL.42.004756

A new technique suitable for generating broadband phase-locked frequency combs in the mid-infrared (mid-IR), based on a degenerate (subharmonic) optical parametric oscillator (OPO), which rigorously downconverts and augments the spectrum of a pump frequency comb, has recently been introduced [1]. For example, an instantaneous mid-IR spectrum of 2.5–3.8 μm was achieved in an OPO based on a 0.5 mm long periodically poled lithium niobate (PPLN) crystal pumped by a mode-locked erbium fiber laser [2]. Quasi-phase-matched (QPM) semiconductors, such as GaAs and GaP, have (i) much deeper mid-IR transparency and (ii) smaller mid-IR group dispersion than PPLN, which is a prerequisite for generating broadband frequency combs. While orientation-patterned (OP) GaAs has already shown great promise for wavelength conversion—both in mid-IR and THz ranges, and from CW to fs formats [3–6], its primary limitation is that it cannot be pumped at $\lambda < 1.8$ μm due to the onset of two-photon absorption. Orientation-patterned gallium phosphide (OP-GaP)—a new QPM material with a larger (and indirect) band gap of 2.26 eV at 300 K—overcomes this limitation. Recently, femtosecond OPOs based on OP-GaP, with pump wavelengths near 1 μm [7], 1.5 μm [8], and 2 μm [9], were demonstrated. With a nonlinear figure of merit d_{eff}^2/n^3, which is similar to that of PPLN (here d_{eff} is the effective nonlinear coefficient and n is the average refractive index), GaP has the advantage of having much smaller mid-IR group velocity dispersion (GVD), which varies from 393 fs^2/mm to −41 fs^2/mm in the 2.5–5 μm spectral range, as compared with −211 fs^2/mm to −3940 fs^2/mm variation for PPLN in the same range.

Here we report an octave-wide OP-GaP-based OPO that is pumped by a telecommunication-range fiber laser and is suitable for producing phase-locked frequency combs in the mid-IR. A schematic of the OPO setup is presented in Fig. 1(a). The pump source was an Er-doped fiber laser from Toptica Inc. (1560 nm central wavelength, 300 mW average power, 80 MHz repetition frequency, and 85 fs pulse duration). We regard this laser as a free-running frequency comb in this work. The compact OPO cavity was composed of a dielectric pump incoupling mirror (M1) with a high transmission (>85%) at 1560 nm and high reflection for the signal/idler wavelengths (>95% at 2.4–4.2 μm and >50% at 2.2–4.9 μm) and three gold-coated mirrors (M2–M4), two of which (M2 and M3) are parabolic with an off-axis angle of 30° and radius curvature in the apex $R = 30$ mm, and one of which (M3) was flat (not shown are four gold-coated folding mirrors to reduce the footprint). A broad-bandwidth gain was provided by a 0.5 mm thick OP-GaP crystal, with a QPM period 46.5 μm, grown by a combination of molecular beam epitaxy (MBE) and low-pressure hydride vapor phase epitaxy [7]. The OP-GaP crystal was mounted at the Brewster's angle (71°), to minimize the reflection of the *p*-polarized signal/idler and pump waves. Inside the crystal, the beams propagated along

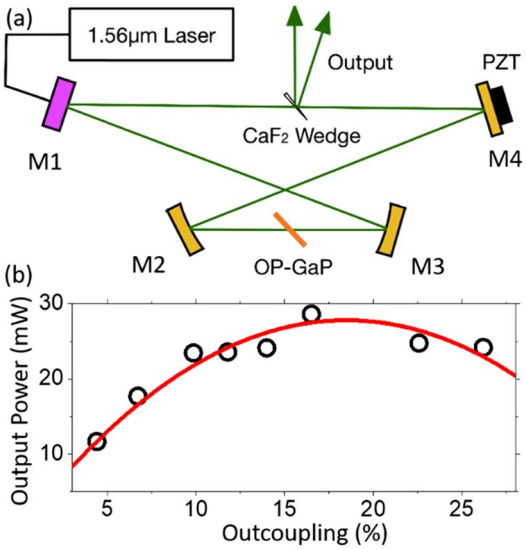

Fig. 1. (a) OPO schematic. M1 is a dielectric mirror that transmits the pump wave and reflects the signal/idler wave of the OPO. The M2 and M3 are parabolic gold-coated mirrors; M4 is a flat gold-coated mirror with a piezoelectric transducer (PZT) for cavity length tuning. (b) The OPO output power from two surfaces of the CaF_2 wedge versus outcoupling strength. The solid curve is a trace for the eye.

−110, and all polarizations were along the 111 direction of GaP.

A CaF_2 wedge (1° angle, average thickness 1.14 mm) was placed in the cavity to (i) compensate, in the first-order approximation, the GVD of GaP (at 3.12 μm degeneracy, GaP has GVD of 280 fs^2/mm and CaF_2 has −122 fs^2/mm) and (ii) for the OPO beam outcoupling via Fresnel reflection.

Figure 2(a) shows the computed overall extra phase delay accumulated per OPO cavity round-trip, as a function of frequency, along with contributions of the GaP crystal, CaF_2 wedge, and dielectric mirror. (Extra phase is the result of the residual group velocity dispersion that causes resonator modes to be slightly nonequidistant. This causes an extra phase accumulated per round trip for each mode. The latter is calculated via double integration, over frequency, of the round-trip group delay dispersion, expressed in fs^2). Our estimate for the extra phase tolerance is ±0.5 rad, which comes from the finesse

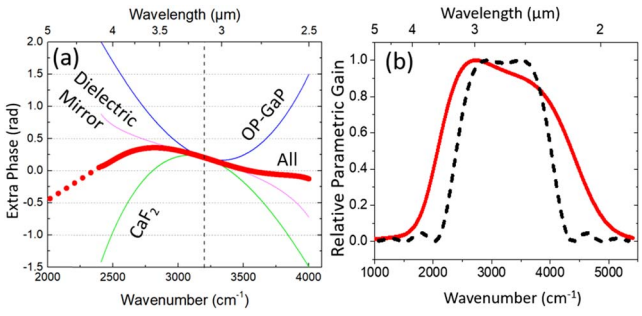

Fig. 2. (a) Computed extra-phase delay per OPO cavity round-trip, as a function of frequency (thick line), along with contributions of the GaP crystal, CaF_2 wedge, and dielectric mirror. (b) The relative parametric gain for the finite pump spectrum (solid line) as compared with that for a monochromatic pump (dashed line).

of the cavity and the available pump power. From Fig. 2(a), one can see that the computed overall round-trip extra phase allows for a spectrum more than one octave wide to be achieved.

Usually, parametric gain of a nonlinear crystal is calculated by assuming a monochromatic pump. Here, we calculated parametric gain by assuming a finite (∼100 nm) FWHM Gaussian spectrum of the pump. The corresponding parametric gain for the 0.5 mm thick OP-GaP used in our OPO is shown as a thick red line in Fig. 2(b), where one can see that the FWHM gain bandwidth is from 2070 to 4370 cm^{-1} (2.28–4.83 μm). The gain curve for a monochromatic pump is also plotted on the same figure for comparison.

The OPO oscillation was achieved by tuning the cavity length using a piezo actuator attached to the mirror M4. The OPO pump threshold was measured to be 14 mW. This low threshold is a result of a doubly resonant performance [1]. Figure 1(b) shows the output power versus outcoupling from the CaF_2 wedge, which was varied by turning the wedge away from the Brewster angle toward normal. The highest mid-IR power (sum of two reflections from CaF_2 surfaces) of 29 mW was achieved at ∼17% outcoupling. The measured OPO pump depletion was 75%.

A doubly resonant OPO oscillates at several discrete cavity lengths (that are close to the synchronous pumping condition), separated in round trip by the wavelength of the pump (1.56 μm) [2]. Switching from one resonant cavity length to another is equivalent to changing, in a step-like fashion, the dispersion in the cavity, which results in the change of the instantaneous spectrum. The OPO output spectrum was measured using a monochromator and a HgCdTe detector. The 2D color-coded intensity plots of Fig. 3(a) represent the output spectra as a function of cavity length detuning. Each horizontal "stripe" corresponds to one of the resonant peaks in the OPO output. The OPO spectrum evolved from degenerate to nondegenerate mode when the cavity was detuned to shorter lengths. The second stripe from the top yields the broadest instantaneous spectrum while still being degenerate.

Continuous operation of the OPO was achieved by locking the cavity length to one of the resonances via the dither-and-lock method [2] involving a PZT actuator and a lock-box (LaseLock from TEM-Messtechnik GmbH). Figure 3(b) shows the broadest measured degenerate OPO spectrum spanning from 2.30 to 4.84 μm (2064–4346 cm^{-1}) at the −25 dB level. This spectrum corresponds to the second stripe from the top on the 2D plot of Fig. 3(a). Although the cavity was purged with dry nitrogen, which reduced the CO_2 concentration to less than 5 ppm and the H_2O concentration to 400 ppm, the spectrum was still affected by the absorption of these two molecules in the measurement system. The top panel of Fig. 3(b) shows the cavity round-trip transmission, corresponding to the above concentrations, averaged over 10 cm^{-1} to match the resolution of the monochromator.

To verify that the octave-wide degenerate spectrum is a single frequency comb, we performed f-to-2f beat measurements in the radio frequency (RF) domain. This experiment allows us to characterize coherence properties of a frequency comb and to stabilize its carrier envelope offset frequency (f_{CEO}). Figure 4 represents a conceptual schematic of our f-to-2f beat experiment. We used two detectors with a spectral window of 10–100 nm, so that one of them (Det. 1, InAs-based) detects the degenerate wavelength at 3.12 μm, while the other

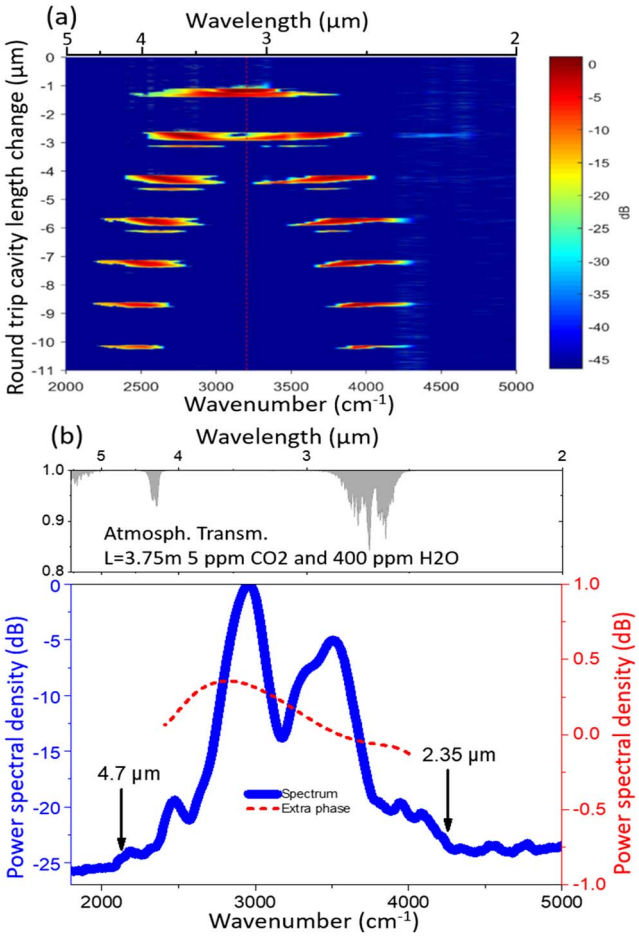

Fig. 3. (a) 2D color intensity plots of the output spectra as the resonator length is detuned. (b) The broadest measured degenerate OPO spectrum (solid line). Also shown is the calculated round-trip cavity extra phase (dashed line). The top panel shows transmission for one cavity round trip for 5 ppm CO_2 and 400 ppm H_2O.

(Det. 2, extended InGaAs-based) detects only a 2.35 μm portion of the spectrum (optical frequency $2f$), which is 3/4 of the degenerate wavelength, such that the second harmonic (SH) of the 4.7 μm part of the spectrum (optical frequency f), parasitically produced in the OP-GaP inside the OPO cavity, would interfere with the 2.35 μm portion of the spectrum. Both detectors were connected to RF spectrum analyzers (RFSA).

When the spectrum is degenerate and less than one octave wide [Fig. 4(a)], we expect Det. 1 to show only one RF peak, which corresponds to the repetition frequency f_{rep}. Det. 2 is expected to provide no signal because the spectrum is not broad enough. As the spectrum becomes broader than an octave [Fig. 4(b)], an RFSA signal should appear from Det. 2 in the form of an f_{rep} peak and satellites that correspond to f-to-$2f$ beats. At the same time, Det. 1 is expected to show only one peak at f_{rep}. Finally, when the spectrum splits into two distinct but overlapping combs (a nondegenerate mode), Det. 1 would see additional beats between the two combs overlapping at degeneracy. The Det. 2 is expected to still produce an f_{rep} peak and show f-to-$2f$ beats, which come from interfering SH of the idler and the OPO signal wave (though now they belong to different combs).

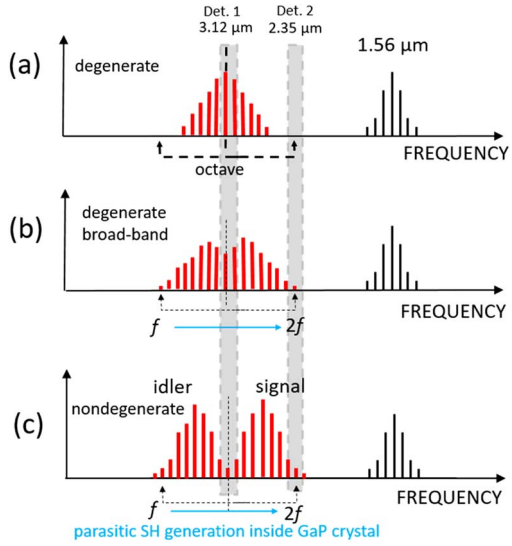

Fig. 4. Conceptual picture of the f-to-$2f$ beat experiment. The spectrum windows for Det. 1 (3.12 μm) and Det. 2 (2.35 μm) are shown as gray dashed boxes. (a) Single comb with less-than-octave-wide spectrum. (b) Single comb with >1 octave-wide spectrum. (c) Nondegenerate scenario with two distinct and overlapping combs. The parasitic SH of the red part of the spectrum in (b), (c), parasitically generated inside the GaP crystal, is expected to interfere with the blue part of the spectrum to produce f-to-$2f$ beats.

The f-to-$2f$ experimental results were close to expectations and are shown in Fig. 5. By switching to different cavity resonances, we were able to vary the spectrum of the OPO from degenerate to nondegenerate, similar to [6], and observe RFSA signals originating from Det. 1 and Det. 2. Figures 5(a)–5(c) show the OPO spectra (linear scale) measured by an FTIR spectrometer, while Figs. 5(d)–5(f) show screenshots of the RFSA for the Det. 1, and Figs. 5(g)–5(i)—for Det. 2. The bandwidth of the RFSA was set to 300 kHz.

Figure 5(a) corresponds to a single comb with a less-than-octave-wide spectrum, while Fig. 5(b) corresponds to a single

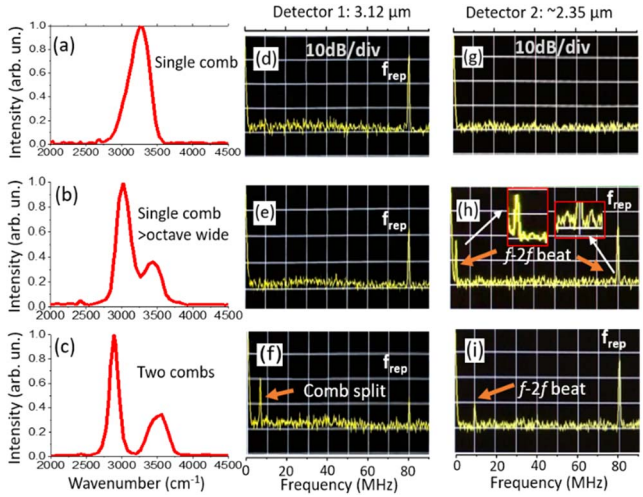

Fig. 5. (a)–(c) Linear-scale optical spectra from an FTIR spectrometer. (d)–(f) Corresponding RF spectra from Det. 1 (3.12 μm). (g)–(i) RF spectra from Det. 2 (2.35 μm).

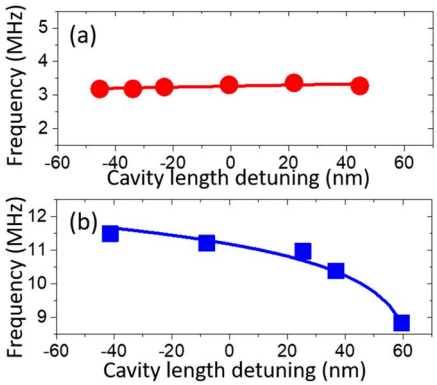

Fig. 6. RF beat frequency versus cavity length detuning from resonance in (a) degenerate scenario and (b) nondegenerate scenario. Solid lines are traces for the eye.

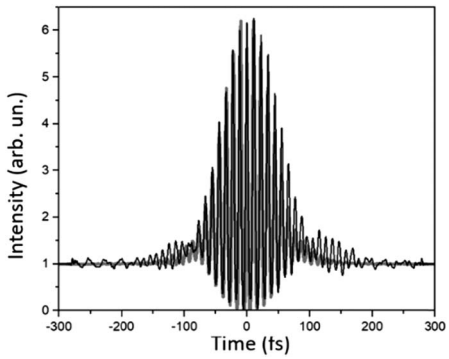

Fig. 7. Second-order interferometric autocorrelation trace (thin black). Simulated curve assuming sech^2 pulse with 70 fs FWHM (thick gray).

comb that reached an octave. In the latter case, Det. 1 shows only one peak at f_{rep} [Fig. 5(e)], which indicates that the OPO output is still one comb. The Det. 2 sees both the f-to-2f beats (at 3 MHz) and the f_{rep} peak. For this scenario, the signal-to-noise ratio for the f-to-2f peak was more than 17 dB. Because our detectors had a bandwidth of 50–60 MHz, the observed RF beats near f_{rep} were much weaker than their low-frequency "mirror-image" counterparts. However, from the second inset on Fig. 5(h), we can still see the two sidebands around f_{rep}, corresponding to f-to-2f beats at 3 MHz. In the case of Fig. 5(c), the OPO is nondegenerate: Det. 1 shows a peak near 6 MHz that suggests a splitting of the OPO combs that overlap at 3.12 μm degeneracy wavelength and produce beats, while Det. 2 shows a peak at 10 MHz due to f-to-2f beats originating from SH of the idler interfering with the signal wave.

To further verify that the f-to-2f beat comes from a single comb in the scenario of Fig. 5(b), we recorded RF beats while slowly detuning the cavity length near resonance at a speed of ~34 nm/s. Because the CEO frequency of the subharmonic OPO is locked to that of the pump [1], that is $f_{CEO,OPO} = f_{CEO,pu}/2$, or $f_{CEO,OPO} = f_{CEO,pu}/2 + f_{rep}/2$, the beat frequency did not change with cavity detuning, as seen from Fig. 6(a) (a small linear slope is possibly due to the drift of CEO of our free running pump source). In contrast, for the nondegenerate scenario in Fig. 5(c), we observed a noticeable RF beat frequency change with the cavity length detuning [Fig. 6(b)] because CEO frequencies for the signal and idler waves are no longer locked together.

Finally, the second-order autocorrelation trace corresponding to the broadest spectrum of Fig. 3(b) was measured with an InGaAs photodiode serving as a two-photon detector and is shown in Fig. 7. Also shown is the simulation trace assuming sech^2 shape and FWHM pulse duration of 70 fs. However, this duration is the upper limit because the pulse was broadened by the dispersion of the optical elements used, such as a long-pass filter, beam splitter, and the focusing lens.

In conclusion, using an orientation-patterned GaP crystal as the gain element, we achieved an octave-wide 2.30–4.84 μm spectrum in a low-threshold (14 mW) subharmonic OPO, pumped by a free-running Er-fiber laser comb. The average comb output power was 29 mW. The spectral span achieved was more than 50% broader, as compared with the prior state-of-the-art based on an Er-fiber-pumped PPLN-based system. Moreover, given the fact that CEO of a degenerate frequency-divide-by-2 OPO is inherently locked to that of the pump laser, the observed f-to-2f frequency beats might be used for self-referencing and frequency comb stabilization of the pump laser itself, with no need for sacrificing laser power for supercontinuum generation.

Funding. Office of Naval Research (ONR) (N00014-15-1-2659); Defense Advanced Research Projects Agency (DARPA) (W31P4Q-15-1-0008); National Science Foundation (NSF) (1144246).

Acknowledgment. Z. L. thanks NSF for support under the Graduate Research Fellowship Program. We also thank Andrey Muraviev for his help in performing experiments.

REFERENCES

1. K. L. Vodopyanov, S. T. Wong, and R. L. Byer, "Infrared frequency comb methods, arrangements and applications," U.S. patent 8,384,990 (February 26, 2013).
2. N. Leindecker, A. Marandi, R. L. Byer, and K. L. Vodopyanov, Opt. Express **19**, 6296 (2011).
3. K. L. Vodopyanov, Laser Photon. Rev. **2**, 11 (2008).
4. J. Kiessling, I. Breunig, P. G. Schunemann, K. Buse, and K. L. Vodopyanov, New J. Phys. **15**, 105014 (2013).
5. V. O. Smolski, S. Vasilyev, P. G. Schunemann, S. B. Mirov, and K. L. Vodopyanov, Opt. Lett. **40**, 2906 (2015).
6. V. O. Smolski, H. Yang, S. D. Gorelov, P. G. Schunemann, and K. L. Vodopyanov, Opt. Lett. **41**, 1388 (2016).
7. L. Maidment, P. G. Schunemann, and D. T. Reid, Opt. Lett. **41**, 4261 (2016).
8. Q. Ru, Z. Loparo, P. G. Schunemann, and K. L. Vodopyanov, *Conference on Lasers and Electro-Optics* (Optical Society of America, 2016), p. STu1Q.6.
9. E. Sorokin, A. Marandi, P. G. Schunemann, M. Fejer, I. T. Sorokina, and R. L. Byer, *High-Brightness Sources and Light-Driven Interactions* (Optical Society of America, 2016), p. MS3C.2.